

found 233.1359.

2-(Trimethylsilyl)bicyclo[6.2.0]deca-2,4,6,8(1)-tetraen-10-methanol 3,5-Dinitrobenzoate (9). In a 10-mL flask was placed the alcohol from above (40 mg, 0.17 mmol) and 5 mL of dry dichloromethane followed by 3,5-dinitrobenzoyl chloride (46 mg, 0.2 mmol), triethylamine (0.1 mL, 0.7 mmol), and a catalytic amount of (dimethylamino)pyridine. The reaction mixture was stirred at room temperature for 1 h, diluted with 50 mL of dichloromethane, washed with water and brine, and dried over Na_2SO_4 . The crude ester obtained after removal of the solvent was crystallized from petroleum ether-ethyl acetate to afford the crystalline 3,5-dinitrobenzoate derivative (70 mg) in 95% yield: mp 102.4 °C; IR (Nujol) 3050, 1720, 1630, 1590, 1380 cm^{-1} ; $^1\text{H NMR}$ (CDCl_3) δ 9.23 (3 H, s), 5.93 (1 H, d, $J = 3.9$), 5.75 (1 H, dd, $J = 11.3, 4.3$), 5.59 (1 H, d, $J = 11.3$), 5.5 (1 H, dd, $J = 11.9, 3.9$), 5.4 (1 H, dd, $J = 11.9, 4.3$), 4.66 (2 H, m), 3.16 (1 H, m), 2.61 (1 H, dd, $J = 13.4, 4.5$), 2.35 (1 H, d, $J = 13.4$), 0.12 (9 H, s); UV (hexane) 210 nm, ϵ 45 000; HRMS calcd for $\text{C}_{21}\text{H}_{22}\text{N}_2\text{O}_6\text{Si}$ 426.1241, found 426.1245. Anal. Calcd for $\text{C}_{21}\text{H}_{22}\text{N}_2\text{O}_6\text{Si}$: C, 59.14; H, 5.19; N, 6.57. Found: C, 59.09; H, 5.22; N, 6.53.

Electrochemistry. Electrochemical measurements were performed by using a BAS-100A electrochemical analyzer. The platinum working electrode was polished and rinsed with ethanol and acetone before each run. The counter electrode was platinum wire. The silver/silver nitrate reference electrode was made from silver wire and 0.1 M silver nitrate in HMPA and was isolated from the electrolyte by a VYCOR bridge. A 0.1 M solution of tetra-*n*-butylammonium perchlorate in HMPA was

used as supporting electrolyte. Ferrocene/ferrocenium internal standard was checked against the reference before and after each measurement. A sample of **8** was weighed into the cell under argon. Supporting electrolyte (10 mL) was added via syringe to form a 1.5 mM solution of **8**.

Quenching Studies. Fluorescence emission spectra of biacetyl (2.6×10^{-2} M in benzene) in the presence of varying concentrations of quencher were recorded on an SLM 48000S spectrofluorometer with excitation at 403 nm. The integrated fluorescence intensity from 400 to 600 nm was used for Φ .

For quenching studies of the cycloaddition of **10** to give **11**, quencher in varying amounts was added to 3 mL of a 0.01 M degassed stock solution of **10** in acetonitrile containing adamantane. Samples were irradiated simultaneously in Pyrex tubes with a 450-W Hanovia lamp for 1.5 h. Samples were analyzed by capillary GC, and the relative amounts of the components were calculated by using the internal standard method.

Acknowledgment. Financial support from the National Science Foundation (CHE 89-96239) is appreciated. Sampath Venimahavan is thanked for obtaining the electrochemical data.

Supplementary Material Available: Tables of positional parameters, anisotropic displacement parameters, bond distances, bond angles, and torsional angles for **9** (9 pages); table of observed and calculated structure factors for **9** (18 pages). Ordering information is given on any current masthead page.

Evidence for Resonance-Assisted Hydrogen Bonding. 2.¹ Intercorrelation between Crystal Structure and Spectroscopic Parameters in Eight Intramolecularly Hydrogen Bonded 1,3-Diaryl-1,3-propanedione Enols

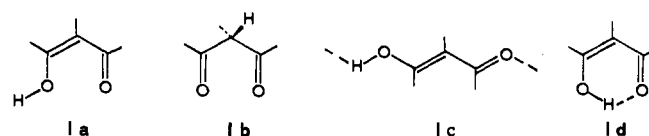
Valerio Bertolasi, Paola Gilli, Valeria Ferretti, and Gastone Gilli*

Contribution from the Centro di Strutturistica Diffraattometrica and Dipartimento di Chimica, Universita' di Ferrara, 44100 Ferrara, Italy. Received October 19, 1990

Abstract: Crystal structure analysis of eight 1,3-diaryl-1,3-propanedione enols has been accomplished with the aim of investigating in more detail the intramolecular hydrogen bond formed by the $\text{HO}-\text{C}=\text{C}-\text{C}=\text{O}$ fragment characterizing β -diketone enols; structural data were correlated with spectroscopic parameters, that is IR $\nu(\text{OH})$ stretching frequencies and $^1\text{H NMR}$ chemical shifts of the enolic proton. Present experimental data show that this hydrogen bond is characterized by the following interrelated features: (i) very short O...O distances (2.432–2.554 Å); (ii) strong delocalization in the heteroconjugated fragment; (iii) lengthening of the O–H bond (to 1.20 Å); (iv) lowering of the $\nu(\text{OH})$ frequencies (2566–2675 cm^{-1}) and downfield shift of the enolic proton resonance (15.3–17.0 ppm). The data can be interpreted by (and are in support of) the RAHB (resonance assisted hydrogen bond) model previously suggested (Gilli, G.; Bellucci, F.; Ferretti, V.; Bertolasi, V. *J. Am. Chem. Soc.* **1989**, *111*, 1023) for explaining the unusual features the hydrogen bond displays in these compounds. It is shown that the model is able to interpret fine structural details such as the general weakening of the intramolecular hydrogen bond caused by electron-donating 1,3-substituents or additional hydrogen bonds accepted by the carbonyl and the preference displayed by the proton for dwelling on the carbonyl oxygen having the smaller negative charge induced both by the nature of 1,3-substituents or by intermolecular hydrogen bonds or short contacts.

Structural chemistry of β -diketones has received increasing attention in the last few years.^{1,2} The interest in the field arises from their being typical sample compounds for studying tautomerism in solution and from the fact that their enol form is stabilized by an intermolecular (Ic) or intramolecular (Id) hydrogen bond

which has unusual characteristics. Furthermore, its energy



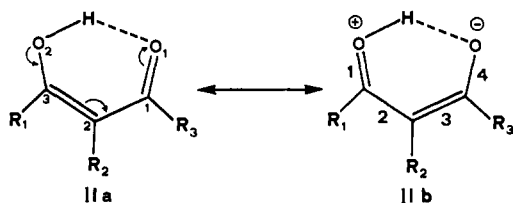
contribution appears to be indispensable to the enolization process itself because, according to a variety of data collected by Emsley^{2a} on malondialdehyde, the non-hydrogen-bonded enol form Ia is some 21 kJ mol^{-1} less stable than the diketone Ib. The role played by the hydrogen bond is such that, with very few exceptions,³ and

(1) Part 1: Gilli, G.; Bellucci, F.; Ferretti, V.; Bertolasi, V. *J. Am. Chem. Soc.* **1989**, *111*, 1023.

(2) (a) Emsley, J. *Struct. Bonding* **1984**, *57*, 147. (b) Etter, M. C.; Vojta, G. M. *J. Mol. Graphics* **1989**, *7*, 3. (c) Emsley, J.; Ma, L. Y. Y.; Bates, P. A.; Motevalli, M.; Hursthouse, M. B. *J. Chem. Soc., Perkin Trans. 2* **1989**, 527. (d) Gilli, G.; Bertolasi, V. In *The Chemistry of Enols*; Rappoport, Z., Ed.; John Wiley & Sons: New York, 1990; Chapter 13.

irrespective of the solvent-dependent tautomeric equilibrium observed in solution,⁴ molecular crystals of β -diketones are found to consist of packings of the enol tautomers stabilized by the stronger intramolecular hydrogen bond, Id. When the compounds are unable to form the intramolecular hydrogen bond, Id, for some steric reason, infinite chains of hydrogen-bonded enol molecules Ic are found.^{2d}

The O-H...O bond formed displays interesting features: (i) the O...O distance may become as short as 2.42–2.43 Å in the intramolecular case^{2a,5} and 2.465 (6) Å in the intermolecular case,⁶ values to be compared with the much longer $d(\text{O}-\text{O})$ distance of 2.74 Å in ice; (ii) the $d(\text{O}-\text{O})$ shortening is associated with an increased delocalization of the π conjugated HO—C=C—C=O system, that is with an increased contribution of the polar form IIb to the ground state of the fragment, which can reach



50% in connection with the shortest intramolecular hydrogen bonds; (iii) the proton position is increasingly shifted toward the centre of the O...O contact with the O-H...O bond strengthening; (iv) at the same time a number of spectroscopic parameters undergo relevant changes, in particular the IR $\nu(\text{OH})$ stretching frequency decreases, the ¹H NMR chemical shift of the enolic proton increases, and the difference of C₁ and C₃ (IIa) chemical shifts in the ¹³C CP/MAS solid state NMR spectra tends to zero.^{2a,4a,7}

In a previous paper¹ we have interpreted such interrelated phenomena by a model, called RAHB (resonance assisted hydrogen bond), which is essentially a synergistic reinforcement of hydrogen bonding and π delocalization. The partial charges generated by resonance on the opposite enol oxygens have the correct sign for strengthening the hydrogen bond with consequent $d(\text{O}-\text{O})$ shortening and $d(\text{O}-\text{H})$ lengthening; the proton, moving toward the negatively charged carbonyl, quenches the opposite charges and allows the π delocalization to proceed further; this imaginary two-stage process continues until the complete π delocalization takes place unless stopped before by the exchange repulsions. By a semiempirical energy model¹ it was shown that the intramolecular hydrogen bond energy was in the range 55–80 kJ mol⁻¹, that is 3–4 times greater than the accepted value in water (some 20 kJ mol⁻¹), and that these figures were in agreement with the available spectroscopic data^{2a,7} and the most recent theoretical evaluations.⁸

It is interesting to note that the enolic proton position has never been found exactly in the middle of the O...O contact even for the strongest hydrogen bonds, suggesting a double well shape of the potential determined for the proton. In solution the exchange between the two positions is extremely fast on the NMR time scale, but temperature-dependent ¹³C NMR studies⁹ on 1,3-disubstituted

propane-1,3-diones ($R_2 = \text{H}$) give some evidence of uneven residence times of the enolic proton in the two minima. The time ratios were 2.38 for $R_1 = \text{CF}_3$ and $R_3 = \text{CH}_3$, 1.47 for $R_1 = \text{Ph}$ and $R_3 = \text{CH}_3$, and 1.08 for $R_1 = \text{CF}_3$ and $R_3 = \text{Ph}$, which defines a $\text{CF}_3 > \text{Ph} > \text{CH}_3$ order of preference of the proton for the carbonyl connected to the more electronegative group. The few crystal structures available confirm this electronegativity rule, as reported in detail in the discussion, indicating that crystals are built up of the tautomer having, in solution, the higher population.

We report here the molecular structure determinations of eight 1,3-diaryl-1,3-propanedione enols together with the characterization of their intramolecular hydrogen bond by solid-state FTIR and solution ¹H NMR spectroscopies with the aim both of establishing a correspondence between the O...O contact distance and the hydrogen bond energy and of gaining some insight into the problem of the effect of different 1,3-substituents on the proton localization.

Experimental Section

The eight compounds were synthesized by the methods given in ref 10 and recrystallized from MeOH, MeOH/CCl₄ mixtures, or amyl acetate. Crystal data and data collections and refinement details are given in Table I. All X-ray diffraction data were collected at room temperature on an Enraf-Nonius CAD4 diffractometer with graphite monochromated Mo K α radiation ($\lambda = 0.71069$ Å) with the $\omega/2\theta$ scan technique. Lattice constants were determined by least-squares fitting of the setting angles of 25 reflections in the range $10 \leq \theta \leq 14^\circ$. Intensities of three standard reflections were measured every 2 h and did not show significant variations for any of the eight compounds investigated. All intensities were collected in the range $2 \leq \theta \leq 27^\circ$ and corrected for Lorentz and polarization effects. Scattering factors were taken from ref 11. Structures were solved by direct methods with the SIR88 system of programs.¹² All other calculations were accomplished by the SDP system of programs and PARST.¹³ All structures were refined by full-matrix least-squares with the exception of compound 7, which was refined in two blocks, one for each independent molecule of the asymmetric unit. Refinement was anisotropic for all non-H atoms and isotropic for H atoms. All H atom positions were found from the ΔF synthesis carried out after the first few cycles of isotropic refinement, including the double positions of the disordered C(16) and C(18) methyl groups of compound 3. An attempt was made to refine the enolic H(1) atom anisotropically. The refinement succeeded for compounds 1–6 and the size and orientation of the final thermal ellipsoids (Figure 1) look reasonable and rather similar to that determined by neutron diffraction at room temperature on dibenzoylmethane.^{14a} The possibility of 2-fold disorder of the enol proton was carefully looked for in the ΔF syntheses and can be excluded for all compounds considered. A selection of geometrical parameters is reported in Table II (also is the supplementary material).

IR spectra were recorded on a Bruker IFS88/FT-IR from KBr pellets and ¹H NMR spectra in a solution of CDCl₃ on a Bruker FT WP-80. Data of $\nu(\text{OH})$ stretching frequencies (cm⁻¹) and chemical shifts of the O-H(1) and C(2)-H(2) protons (ppm) are reported in Table III. The assignment of the $\nu(\text{OH})$ stretching frequency to the weak band in the range 2580–2680 cm⁻¹ was done according to a previous interpretation of the spectra of acetylacetone and dibenzoylmethane.¹⁵

(9) Lazaar, K. I.; Bauer, S. H. *J. Phys. Chem.* **1983**, *87*, 2411.

(10) (a) Barnes, R. P.; Spriggs, A. S. *J. Am. Chem. Soc.* **1945**, *67*, 134.

(b) Barnes, R. P.; Sneed, J. L. *J. Am. Chem. Soc.* **1945**, *67*, 138. (c) Barnes, R. P.; Pinkney, G. E.; Da Costa, W. A. *J. Am. Chem. Soc.* **1947**, *69*, 3129.

(d) Barnes, R. P.; Reed, G. W. *J. Am. Chem. Soc.* **1947**, *69*, 3132. (e) Dayer, F.; Dao, H. L.; Gold, H.; Rodé-Gowald, H.; Dahn, H. *Helv. Chim. Acta* **1974**, *57*, 2201. (f) Kohler, E. P.; Barnes, R. P. *J. Am. Chem. Soc.* **1933**, *55*, 690.

(g) Wieland, H. *Ber.* **1904**, *37*, 1148.

(11) *International Tables for X-Ray Crystallography*; Kynoch Press: Birmingham, U.K., 1974; Vol. 4, p 71.

(12) Burla, M. C.; Camalli, M.; Cascarano, G.; Giacovazzo, C.; Polidori, G.; Spagna, R.; Viterbo, D. SIR88. A Direct-Methods Program for the Automatic Solution of Crystal Structures. *J. Appl. Cryst.* **1989**, *22*, 389.

(13) (a) Frenz, B. A. *SDP. A Structure Determination Package*. College Station, Texas; Enraf-Nonius: Delft, The Netherlands, 1978. (b) Nardelli, M. *Comput. Chem.* **1983**, *7*, 95.

(14) (a) Jones, R. D. G. *Acta Crystallogr. Sect. B* **1976**, *32*, 1807. The structure of DBM has been determined also by X-ray analysis: (b) Williams, D. E. *Acta Crystallogr.* **1966**, *21*, 340. Hollander, F. J.; Templeton, D. H.; Zalkin, A. *Acta Crystallogr. Sect. B* **1973**, *29*, 1552. The X-ray structure of a polymorphic phase also has been reported: (c) Etter, M. C.; Jahn, D. A.; Urbanczyk-Lipkowska, Z. *Acta Crystallogr. Sect. C* **1987**, *43*, 260.

(3) (a) Emsley, J.; Freeman, N. J.; Hursthouse, M. B.; Bates, P. A. *J. Mol. Struct.* **1987**, *161*, 181. (b) Mullica, D. F.; Karban, J. W.; Grossie, D. A. *Acta Crystallogr. Sect. C* **1987**, *43*, 601.

(4) (a) Floris, B. In *The Chemistry of Enols*; Rappoport, Z., Ed.; John Wiley & Sons: New York, 1990; Chapter 4. (b) Toulec, J. In *The Chemistry of Enols*; Rappoport, Z., Ed.; John Wiley & Sons: New York, 1990; Chapter 6.

(5) (a) Görblitz, C. H.; Mostad, A.; Pedersen, U.; Rasmussen, P. B.; Lawesson, S. O. *Acta Chem. Scand. Ser. B* **1986**, *40*, 420. (b) Jones, R. D. G.; Power, L. F. *Acta Crystallogr. Sect. B* **1976**, *32*, 1801.

(6) Bideau, J. P.; Bravic, G.; Filhol, A. *Acta Crystallogr. Sect. B* **1977**, *3847*.

(7) (a) Ogoshi, H.; Yoshida, Z. *Chem. Commun.* **1970**, 176. (b) Kopleva, T. S.; Shigorin, D. N. *Russ. J. Phys. Chem.* **1974**, *48*, 312. (c) Etter, M. C.; Vojta, G. M. Private communication.

(8) (a) Bicerano, J.; Schaefer, H. F., III; Miller, W. H. *J. Am. Chem. Soc.* **1983**, *105*, 2550. (b) Frisch, M. J.; Schneiner, A. C.; Schaefer, H. F., III; Binkley, J. S. *J. Chem. Phys.* **1985**, *82*, 4194.

Table I. Crystal Data

compd	1	2	3	4	5	6	7	8
name	1-phenyl-3-(<i>p</i> -nitrophenyl)-1,3-propanedione enol	1-phenyl-3-(<i>p</i> -methoxyphenyl)-1,3-propanedione enol	1-phenyl-3-mesityl-1,3-propanedione enol	1-(<i>p</i> -nitrophenyl)-3-mesityl-1,3-propanedione enol	1-mesityl-3-(<i>m</i> -nitrophenyl)-1,3-propanedione enol	1-mesityl-3-(<i>o</i> -nitrophenyl)-1,3-propanedione enol	1-(<i>p</i> -methoxyphenyl)-3-(<i>m</i> -nitrophenyl)-1,3-propanedione enol	1-mesityl-3-(<i>p</i> -methoxyphenyl)-1,3-propanedione enol
formula	C ₁₅ H ₁₁ O ₄ N	C ₁₆ H ₁₄ O ₃	C ₁₈ H ₁₈ O ₂	C ₁₈ H ₁₇ O ₄ N	C ₁₈ H ₁₇ O ₄ N	C ₁₈ H ₁₇ O ₄ N	C ₁₆ H ₁₃ O ₅ N	C ₁₉ H ₂₀ O ₃
<i>M_r</i>	269.26	254.29	266.34	311.34	311.34	311.34	299.28	296.37
space group	<i>P2₁/c</i>	<i>Pbca</i>	<i>P2₁2₁2₁</i>	<i>P2₁/c</i>	<i>P2₁/n</i>	<i>Pbca</i>	<i>P2₁/n</i>	<i>P2₁2₁2₁</i>
cryst syst	monoclinic	orthorombic	orthorombic	monoclinic	monoclinic	orthorombic	monoclinic	orthorombic
<i>a</i> , Å	8.306 (2)	7.750 (2)	6.910 (2)	10.632 (7)	8.552 (2)	10.387 (2)	13.050 (3)	6.402 (2)
<i>b</i> , Å	6.785 (4)	10.797 (1)	7.113 (1)	14.228 (1)	13.613 (2)	15.458 (2)	15.975 (3)	7.206 (1)
<i>c</i> , Å	22.233 (4)	30.335 (4)	30.963 (4)	11.324 (2)	13.864 (1)	19.676 (2)	14.425 (6)	35.395 (6)
β , deg	92.81 (2)			105.12 (1)	91.78 (1)		111.16 (3)	
<i>V</i> , Å ³	1251.4	2538.2	1522.7	1653.8	1613.3	3159.2	2804.5	1632.8
<i>Z</i>	4	8	4	4	4	8	8	4
<i>D_c</i> , g cm ⁻³	1.43	1.33	1.16	1.25	1.28	1.31	1.42	1.20
<i>F</i> (000)	560	1072	568	656	656	1312	1248	632
μ (Mo K α), cm ⁻¹	0.98	0.85	0.69	0.83	0.85	0.87	1.00	0.75
crystal size, nm ³	0.12 × 0.17 × 0.52	0.17 × 0.21 × 0.33	0.17 × 0.26 × 0.26	0.21 × 0.19 × 0.55	0.14 × 0.14 × 0.50	0.26 × 0.45 × 0.48	0.14 × 0.17 × 0.45	0.16 × 0.36 × 0.55
independent reflcns	2714	2750	2137	3602	3520	3434	6113	2750
obsd reflcns	1239 [<i>I</i> ≥ 2.5 σ (<i>I</i>)]	1365 [<i>I</i> ≥ 3 σ (<i>I</i>)]	1076 [<i>I</i> ≥ 2 σ (<i>I</i>)]	1560 [<i>I</i> ≥ 3 σ (<i>I</i>)]	1717 [<i>I</i> ≥ 3 σ (<i>I</i>)]	2119 [<i>I</i> ≥ 3 σ (<i>I</i>)]	1869 [<i>I</i> ≥ 2 σ (<i>I</i>)]	1640 [<i>I</i> ≥ 2 σ (<i>I</i>)]
<i>R</i> ^a	0.052	0.036	0.043	0.039	0.042	0.043	0.055	0.045
<i>R_w</i> ^b	0.069	0.044	0.056	0.047	0.052	0.056	0.053	0.059
<i>P</i> ^c	0.08	0.05	0.06	0.04	0.05	0.05	0.03	0.05
<i>n/p</i>	5.51	5.86	4.85	5.55	6.11	7.54	5.18	5.88
max shift/error	0.06	0.52	0.35	0.16	0.48	0.45	0.22	0.08
largest ΔF peak, e Å ⁻³	0.24	0.13	0.12	0.11	0.15	0.17	0.17	0.17
GOF ^d	1.36	1.27	1.42	1.49	1.44	1.64	1.71	1.69
no. of variables (last cycle)	225	233	222	281	281	281	361	279

$$^a R = \sum[|F_o| - |F_c|] / \sum|F_o|. \quad ^b R_w = [\sum w(|F_o| - |F_c|)^2 / \sum w|F_o|^2]^{1/2}. \quad ^c \text{Weighting scheme: } w = 4F_o^2 / [\sigma^2(F_o^2) + (PF_o^2)^2]. \quad ^d \text{GOF} = [\sum w(|F_o| - |F_c|)^2 / (n - p)]^{1/2}.$$

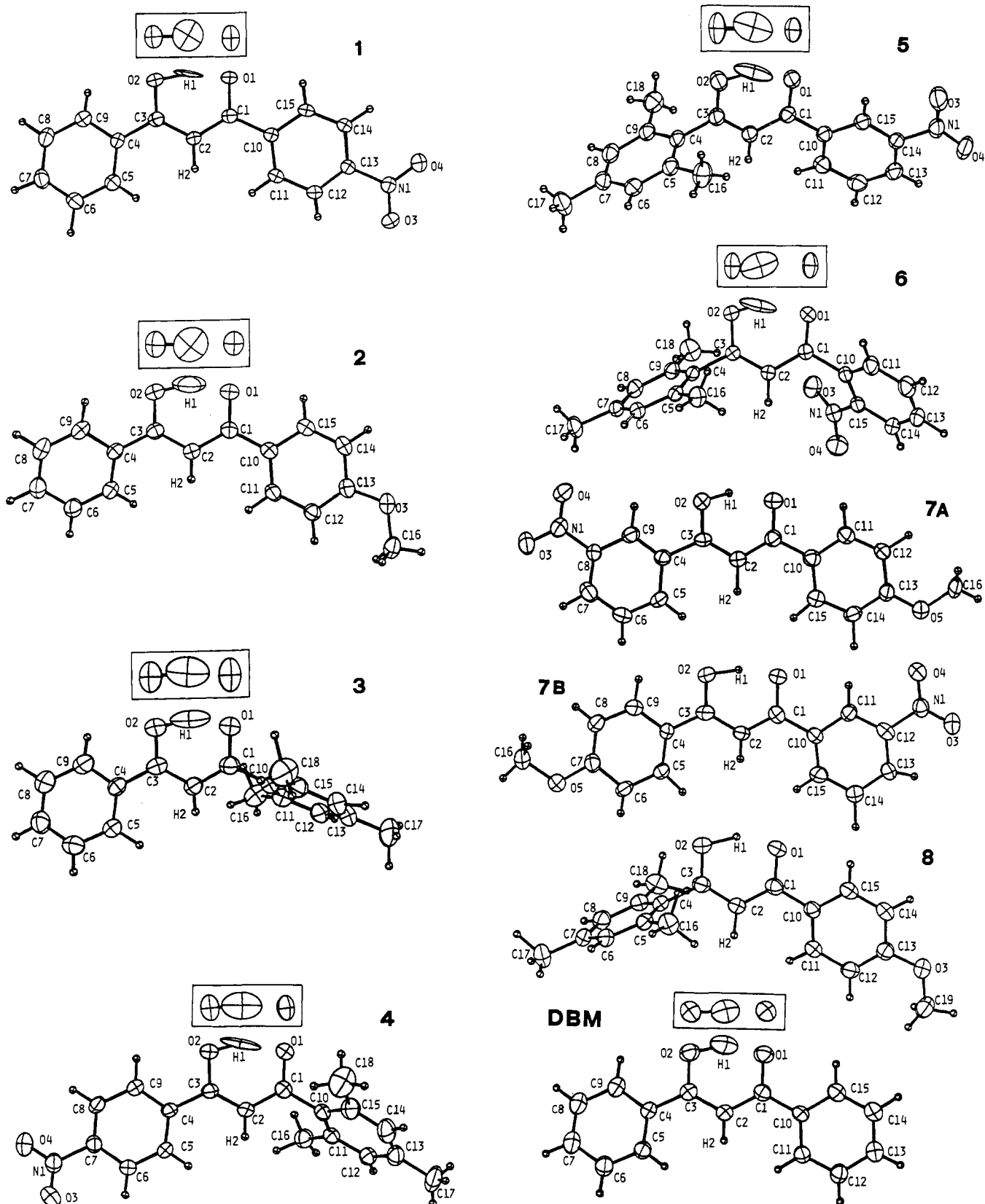


Figure 1. ORTEP¹⁶ views of molecules 1–8 and dibenzoylmethane (DBM)^{14a} showing the thermal ellipsoids at 30% probability and approximately projected on the mean plane of the β -diketone group. The small inserts show the orthogonal view of the thermal ellipsoids of the O–H–O fragment.

Description of the Structures

The ORTEP¹⁶ views of the eight molecules and of the parent molecule dibenzoylmethane (DBM)^{14a} displaying the thermal ellipsoids at 30% probability are shown in Figure 1. Molecules are nearly projected on the mean plane of the β -diketone enol

group and the small inserts show the orthogonal views of the O(2)–H(1)–O(1) anisotropic thermal ellipsoids for the present X-ray structures 1–6 and for DBM, determined by room temperature neutron diffraction.^{14a} Even making proper allowance for the low accuracy of the proton X-ray ellipsoids, they seem to show some systematic aspects. The two oxygens by themselves

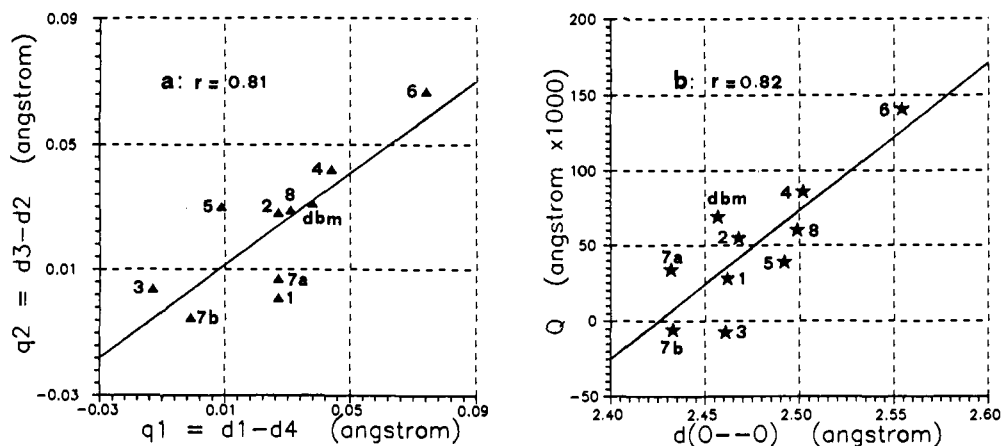


Figure 2. (a) Scatter plot of $q_2 = d_3 - d_2$ vs $q_1 = d_1 - d_4$ (Å) for compounds 1–8 and dibenzoylmethane (DBM);^{14a} (b) scatter plot of $Q = q_1 + q_2$ vs $d(\text{O}--\text{O})$ (Å) for the same compounds as in part a. Linear regression coefficients (r) are given on the figures.

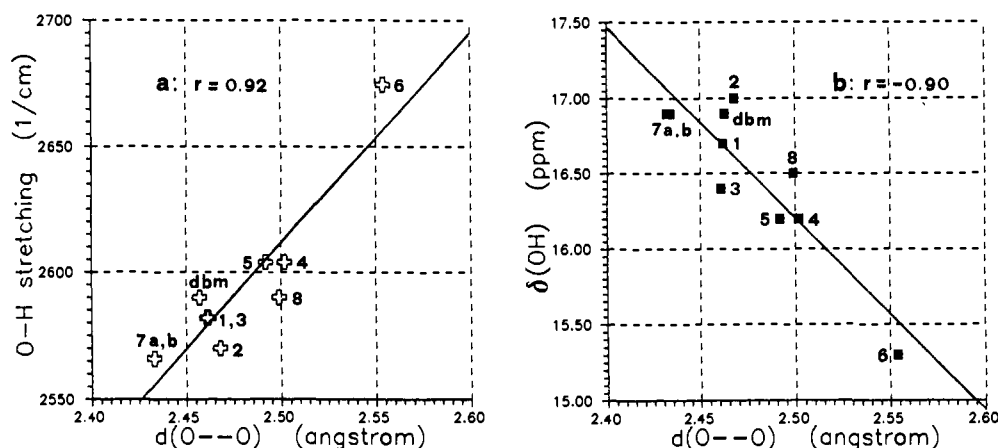


Figure 3. (a) Scatter plot of the IR $\nu(\text{OH})$ stretching frequency (cm^{-1}) vs $d(\text{O}--\text{O})$ (Å) for compounds of Figure 2a; (b) scatter plot of the ^1H NMR chemical shift of the enolic proton, $\delta(\text{OH})$ (ppm) vs $d(\text{O}--\text{O})$ (Å) for the same compounds as in part a. Linear regression coefficients (r) are given on the figures.

have a greater out-of-plane vibration, which is reflected by an analogous motion of the interleaving hydrogen; the two orthogonal in-plane hydrogen vibrations are quite dissimilar and indicative of a strong anisotropy of the potential experienced by the proton; they are consistent with a shallow potential on the line connecting the two oxygens and a steep one perpendicular to it. The conformations of the phenyl groups with respect to the mean plane $\Phi_1 = \text{O}(1), \text{C}(1), \text{C}(2), \text{C}(3), \text{O}(2)$ are reported in Table II as angles formed with the least-squares planes Φ_2 and Φ_3 passing through the six ring C atoms and connected respectively to the enol and carbonyl groups. Phenyl groups show a definite tendency to be coplanar with the β -diketone enol fragment, the out-of-plane rotations being associated with steric hindrances of the ortho substituents. An interesting situation arises in compound 6, where the ortho nitro group interacts with the carbonyl C(1) atom by a very short charge-transfer contact ($\text{O}(3)-\text{C}(1)$ distance of 2.724 (2) Å) which is some 0.50 Å shorter than the sum of the van der Waals radii. The coplanarity of the phenyl groups cannot be due to a phenyl participation in the keto-enol π conjugated system since the carbon-carbon 5 and 6 distances of Table II (on average 1.48 [1] Å) do not show any systematic dependence on the phenyl torsion angles. The planarity could be attributed to other factors

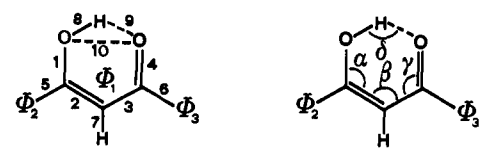
as well, such as the greater packing efficiency of planar objects or an energetically favorable C-H...O interaction of the C=O and C=O oxygens with the ortho phenyl hydrogens.

All crystals are built up of discrete molecular units without intermolecular hydrogen bonds or significantly short contacts. The outstanding feature of these molecules is that the β -diketone enol group forms in all cases a very short intramolecular $\text{O}(2)-\text{H}(1)-\text{O}(1)$ hydrogen bond [$d(\text{O}--\text{O})$ in the range 2.432–2.554 Å]. Table III summarizes the relevant data. The shortening of $d(\text{O}--\text{O})$ and the lengthening of $d(\text{O}-\text{H})$ are direct indicators of the strength of the hydrogen bond. The decrease of the stretching $\nu(\text{OH})$ IR frequency and the downfield shifts of the $\delta(\text{O}-\text{H})$ and $\delta(\text{C}(2)-\text{H})$ NMR peaks are also indicative of such a strength. Some equations relating the stretching $\nu(\text{O}-\text{H})$ frequency to the hydrogen bond energy in these compounds have been proposed and we have chosen the one given by Kopleva and Shigorin,^{7b} which is $E_{\text{HB}} = 245.9 (\nu_0 - \nu) / \nu_0 \text{ kJ mol}^{-1}$, where ν_0 is the stretching frequency in the absence of the hydrogen bond, which is 3640 cm^{-1} . Values of E_{HB} are also given in Table III.

No direct indicator of the π delocalization in the β -diketone fragment is available, but the symmetry coordinates corresponding to its antisymmetrical in-plane vibration can be used¹, defined as $q_1 = d_1 - d_4$ and $q_2 = d_3 - d_2$. As these two coordinates are actually interconnected as shown in Figure 2a by a correlation coefficient of 0.82, a unique antisymmetrical vibration coordinate^{1,2d} $Q = q_1 + q_2$ can be considered to represent the π delocalization of the $\text{O}-\text{C}=\text{C}-\text{C}=\text{O}$ heterodiene as a whole. Since the standard bond distances in the absence of π delocalization¹⁷ are d_1 (C-O) = 1.37 Å, d_2 (C=C) = 1.33 Å, d_3 (C-C) = 1.48 Å, and d_4 (C=O) = 1.20 Å, Q can range from +0.320 for the

(15) (a) Ogoshi, H.; Nakamoto, K. *J. Chem. Phys.* **1966**, *45*, 3113. (b) Tayyari, S. F.; Zeegers-Huyskens, Th.; Wood, J. L. *Spectrochim. Acta* **1979**, *35*, 1265.

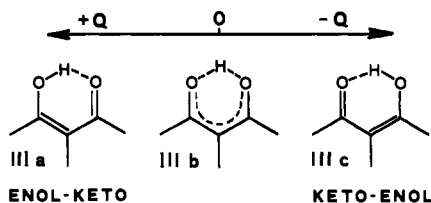
(16) Johnson, C. K. *ORTEP II. A Fortran Thermal-Ellipsoids Plot Program for Crystal Structures Illustrations*; Report ORLN-5138, Oak Ridge National Laboratory, Oak Ridge: TN, 1976.

Table II. Selected Distances (Å), Bond and Torsion Angles and Angles between Least-Squares Planes (deg) for Compounds 1–8^a


compd	1	2	3	4	5	6	7A	7B	8
(a) Distances									
1, d_1	1.313 (4)	1.304 (2)	1.281 (4)	1.309 (3)	1.287 (3)	1.321 (2)	1.305 (6)	1.289 (5)	1.300 (3)
2, d_2	1.391 (4)	1.380 (3)	1.380 (4)	1.367 (3)	1.372 (4)	1.357 (2)	1.382 (7)	1.386 (7)	1.381 (3)
3, d_3	1.397 (4)	1.408 (3)	1.384 (4)	1.409 (4)	1.402 (4)	1.424 (3)	1.389 (7)	1.381 (7)	1.410 (3)
4, d_4	1.288 (4)	1.278 (2)	1.294 (4)	1.265 (3)	1.278 (3)	1.247 (2)	1.278 (6)	1.290 (6)	1.269 (3)
5	1.465 (4)	1.473 (3)	1.480 (4)	1.475 (2)	1.491 (4)	1.486 (2)	1.491 (7)	1.464 (7)	1.484 (3)
6	1.493 (4)	1.472 (3)	1.469 (4)	1.492 (4)	1.481 (3)	1.502 (2)	1.484 (7)	1.462 (7)	1.478 (3)
7	1.01 (3)	0.92 (2)	0.86 (2)	0.92 (2)	0.93 (2)	0.97 (2)	1.11 (5)	0.87 (3)	0.98 (2)
8, $d(\text{O}-\text{H})$	1.12 (4)	1.15 (3)	1.20 (6)	1.07 (4)	1.20 (3)	0.91 (3)	0.98 (3)	1.10 (6)	1.16 (3)
9, $d(\text{H}-\text{O})$	1.38 (4)	1.37 (3)	1.33 (5)	1.49 (4)	1.35 (3)	1.70 (4)	1.53 (3)	1.39 (6)	1.42 (3)
10, $d(\text{O}-\text{O})$	2.465 (3)	2.470 (2)	2.461 (3)	2.502 (2)	2.492 (2)	2.554 (2)	2.432 (4)	2.434 (4)	2.499 (3)
(b) Angles									
1–2, α	120.1 (3)	120.4 (2)	120.7 (3)	120.4 (2)	120.7 (2)	122.0 (2)	121.2 (4)	118.3 (4)	121.5 (2)
2–3, β	120.9 (3)	121.6 (2)	121.5 (3)	122.1 (2)	121.6 (2)	121.3 (2)	119.4 (4)	123.1 (4)	120.8 (2)
3–4, γ	120.6 (2)	119.5 (2)	119.9 (3)	120.6 (2)	120.7 (2)	122.5 (2)	121.2 (4)	118.6 (4)	120.8 (2)
1–8	98 (2)	101 (1)	102 (2)	102 (2)	101 (2)	104 (2)	104 (2)	100 (3)	104 (2)
8–9, δ	162 (3)	156 (2)	152 (4)	155 (2)	156 (2)	153 (2)	150 (3)	155 (6)	150 (3)
(c) Torsion Angles									
4–3–2	0.3 (5)	–4.3 (3)	3.1 (4)	1.8 (4)	–2.5 (4)	0.2 (3)	2.1 (7)	–2.0 (7)	2.2 (4)
3–2–1	0.2 (5)	3.2 (3)	–1.4 (4)	0.0 (3)	4.6 (4)	–2.4 (3)	–1.3 (7)	–0.7 (7)	0.8 (4)
2–1–8	3 (2)	–2 (1)	6 (2)	3 (2)	0 (2)	3 (2)	11 (2)	–8 (3)	0 (2)
(d) Angles between Planes									
$\Phi_1-\Phi_2$	11.4 (1)	26.5 (1)	7.0 (1)	4.5 (1)	82.5 (1)	72.9 (1)	4.0 (2)	8.3 (1)	74.7 (1)
$\Phi_1-\Phi_3$	8.1 (1)	5.5 (1)	78.2 (1)	117.7 (1)	24.7 (1)	56.6 (1)	5.0 (2)	4.2 (2)	18.3 (1)
$\Phi_2-\Phi_3$	17.5 (1)	31.0 (1)	83.1 (1)	114.0 (1)	91.4 (1)	100.7 (1)	3.8 (2)	8.9 (1)	87.2 (1)

^a Esd's in parentheses and symbols according to the scheme shown.

enol-keto form IIIa to -0.320 \AA for the keto-enol form IIIc, being exactly zero only for the fully π delocalized form IIIB. Alter-



natively, the diene geometry can be described as a linear combination of the two forms according to λ (enol-keto) + $(1 - \lambda)$ (keto-enol), where the coupling parameter λ ¹⁸ is calculated to be $\lambda = (1 - Q/3.320)/2$.

Discussion

Figure 2b reports the scatter plot of Q vs $d(\text{O}-\text{O})$ ($r = 0.82$) and shows that very short $d(\text{O}-\text{O})$ values (and therefore very strong hydrogen bonds) are associated with larger π delocalizations. Similar plots have been reported elsewhere^{1,2d} for a larger selection of compounds spanning rather wider intervals of q ($0 \leq q_1, q_2 \leq 0.14 \text{ \AA}$), Q ($0 \leq Q \leq 0.25 \text{ \AA}$), and $\text{O}-\text{O}$ distances ($2.42 \leq d(\text{O}-\text{O}) \leq 2.65 \text{ \AA}$); comparison of parts a and b of Figure 2 with these other plots shows that the dibenzoylmethane derivatives considered here are among the most delocalized compounds (small q_1, q_2 , and Q values) and have the shortest $d(\text{O}-\text{O})$ distances. The $d(\text{O}-\text{H})$ and $d(\text{H}-\text{O})$ values (Tables II and III, Figure 4)

display a systematic trend. Neglecting the values for compound 7, which are barely reliable as far as the proton position is concerned, it is seen that both $d(\text{O}-\text{H})$ and $d(\text{H}-\text{O})$ depend on $d(\text{O}-\text{O})$. These values are 0.91 (3) and 1.70 (4) Å for compound 6, having the largest interoxygen distance (2.554 (2) Å), but abruptly change to 1.11 [5] and 1.45 [5] Å, on average, when $d(\text{O}-\text{O})$ becomes 2.50 Å (compounds 4 and 8). For $d(\text{O}-\text{O})$ values shorter than 2.50 Å the two $d(\text{O}-\text{H})$ and $d(\text{H}-\text{O})$ distances become, on average, 1.17 [3] and 1.35 [2] Å (compounds 1, 2, 3, 5), values strictly comparable with those determined by neutron diffraction in DBM^{14a} of 1.161 (9) and 1.360 (9) Å. The general trend of $\text{O}-\text{H}$ and $\text{H}-\text{O}$ distances is displayed in Figure 4, where it is superimposed to the analogous values found in the other 18 β -diketone enols studied in our previous paper.¹

The dependence of the oxygen-hydrogen distances from $d(\text{O}-\text{O})$ is reflected by the scatter plots $\nu(\text{O}-\text{H})$ vs $d(\text{O}-\text{O})$ ($r = 0.92$, Figure 3a) and $\delta(\text{OH})$ vs $d(\text{O}-\text{O})$ ($r = -0.90$, Figure 3b).¹⁹ The lowering of the $\nu(\text{O}-\text{H})$ stretching frequency and the deshielding of the hydroxyl proton, associated with the $d(\text{O}-\text{O})$

(19) The quantity $d(\text{O}-\text{O})$ has been taken as the common abscissa of Figures 2b, 3a, and 3b because it is the hydrogen bond parameter determined with the highest accuracy by X-ray analysis, and a linear dependence of $\nu(\text{OH})$ and $\delta(\text{OH})$ from $d(\text{O}-\text{O})$ was assumed in view of the small $d(\text{O}-\text{O})$ range determined. It is known from studies on ortho-substituted phenols that $\nu(\text{OH})$ and $\delta(\text{OH})$ change linearly, within experimental error, with E_{HB} , the energy of the hydrogen bond (Schaefer, T. *J. Phys. Chem.* 1975, 79, 1888. Takasuka, M.; Matsui, Y. *J. Chem. Soc. Perkin Trans. 2* 1979, 1743). Though E_{HB} can be calculated according to a well-known semiempirical model (Lippincott, E. R.; Schroeder, R. *J. Chem. Phys.* 1955, 23, 1099. Schroeder, R.; Lippincott, E. R. *J. Phys. Chem.* 1957, 61, 921) to decrease almost exponentially with the decreasing $d(\text{O}-\text{O})$, it can be shown that the function is strictly linear within the present interval of $d(\text{O}-\text{O})$ (2.43–2.56 Å). Accordingly, a linear dependence of $\nu(\text{OH})$ and $\delta(\text{OH})$ on $d(\text{O}-\text{O})$ should also be expected. This conclusion is confirmed by the experimental $\nu(\text{OH})$ vs $d(\text{O}-\text{O})$ curve reported by Novak (Novak, A. *Struct. Bonding* 1974, 18, 177) for a variety of strong $\text{O}-\text{H} \cdots \text{O}$ hydrogen bonds and which shows a linear behavior in the interval $2.42 \leq d(\text{O}-\text{O}) \leq 2.60 \text{ \AA}$.

(17) Allen, F. H.; Kennard, O.; Watson, D. G.; Brammer, L.; Orpen, A. G.; Taylor, R. *J. Chem. Soc. Perkin Trans. 2* 1987, S1.

(18) Kirkwood, J. D. In *Theory of Liquids*; Adler, B. J., Ed.; Gordon and Breach: New York, 1968.

Table III. Summary of Crystal and ¹H NMR and IR Spectroscopic Data for Dibenzoylmethane (DBM^{14a}) and Compounds 1-8 Ordered for Decreasing O...O Distances^a

	<i>d</i> (O...O), Å	<i>d</i> (O-H), Å	<i>d</i> (H...O), Å	$q_1 = d_1 - d_4$, Å	$q_2 = d_3 - d_2$, Å	$Q = q_1 + q_2$, Å	λ , Å	ν (O-H), cm ⁻¹	E_{HB} , kJ/mol	δ (C-H), ppm	δ (O-H), ppm	$\sum s(\text{C=O})$	$\sum s(\text{C-OH})$	$\Delta \Sigma$
6	2.554	0.91	1.70	0.074	0.067	0.141	0.479	2675	-65.3	5.93	15.3	0.018	0.011	0.007
4	2.502	1.07	1.49	0.044	0.042	0.086	0.487	2604	-69.9	6.38	16.2	0.025	0.016	0.009
8	2.499	1.16	1.42	0.031	0.029	0.060	0.491	2590	-71.1	6.25	16.5	0.023	0.021	0.002
5	2.492	1.20	1.35	0.009	0.030	0.039	0.494	2604	-69.9	6.40	16.2	0.020	0.004	0.016
2	2.470	1.15	1.37	0.026	0.028	0.054	0.492	2570	-72.4	6.83	17.0	0.029	0.017	0.012
1	2.465	1.12	1.38	0.025	0.006	0.031	0.495	2582	-71.5	6.90	16.7	0.035	0.020	0.015
DBM	2.463	1.16	1.36	0.038	0.031	0.069	0.490	2590	-71.1	6.9	16.9	0.040	0.044	-0.004
3	2.461	1.20	1.33	-0.013	0.004	-0.007	0.501	2582	-71.5	6.35	16.4	0.027	0.030	-0.003
7B	2.434	1.10	1.39	-0.001	-0.005	-0.006	0.501	2566	-72.8	6.84	16.9	0.030	0.030	0.000
7A	2.432	0.98	1.53	0.027	0.007	0.034	0.495	2566	-72.8	6.84	16.9	0.028	0.039	-0.011

^a ν (O-H) is the O-H stretching frequency, δ (C-H) and δ (O-H) the chemical shifts of the vinylic and enolic proton, respectively, E_{HB} is the H bond energy calculated as $E_{\text{HB}} = 245.9 (\Delta\nu/3640)$ (see text), λ is the coupling parameter calculated as $\lambda = (1 - Q/3.320)/2$ (see text), $\sum s(\text{C=O})$ and $\sum s(\text{C-OH})$ are the sums of the bond valence contributions for the ketonic and enolic oxygens, respectively, and $\Delta \Sigma$ are their differences.

shortening, are both indicative of the strengthening of the hydrogen bond and consequent weakening of the O-H bond. The hydrogen bond is abnormally strong in comparison with the usual O-H...O bonds (≈ 20 kJ mol⁻¹) as shown by the energies calculated from the ν (O-H) frequencies^{7b} (Table III), being 65.9 kJ mol⁻¹ for compound 6, having the larger *d*(O...O) distance, and assuming values in the range 69.9–72.8 kJ mol⁻¹ with the decrease of *d*(O...O) from 2.502 to 2.432 Å. It might be remarked that the δ (O-H) shifts measured in CDCl₃ solutions display the same trend as the solid-state properties *d*(O...O), *d*(O-H), and ν (O-H), showing that the intramolecular hydrogen bond has essentially the same length in both the solid and liquid state, in spite of the different situation experienced by the proton in the two cases (frozen in a single position in the solid, and rapidly exchanging between two nearly equivalent minima in solution).

All present data are consistent with what was foreseeable from our previous RAHB model¹ because of the strict intercorrelation between *d*(O...O) distances and π system delocalizations. In all the molecules considered both π delocalization and hydrogen bond strength are near the maximum values observable in β -diketone enols and the variation range is, accordingly, rather limited. For comparison, in β -keto esters, which are known to enolize less readily than β -diketones, *d*(O...O) values are in the range 2.52–2.65 Å and *Q* is, on average, as large as 0.23 Å.^{2d}

As far as the O-H bond is concerned, present findings suggest that a definite O-H lengthening is achievable only for the strongest intramolecular hydrogen bonds having *d*(O...O) distances not longer than 2.50 Å (see Figure 4). In all crystal structures the proton is observed to occupy a slightly asymmetric position,²⁰ confirming the idea of a double minimum potential and in agreement with all known solid state and solution spectroscopic data.^{2a,d} It has been hypothesized that there are theoretical reasons for such a dissymmetry even in symmetrically substituted compounds, arising from a second-order Jahn-Teller distortion.²¹ Furthermore, there is no indication of disordered proton positions between the two minima in crystals. This has been observed in some cases^{2b,22} which, however, all show some peculiarities. In naphthazarin C^{22a} and curcumin^{22b} the intramolecular hydrogen bond is embedded in a net of other intermolecular bonds involving the two enol oxygens and in citrinin^{22c} two β -diketone enol groups are coupled through a common C-C bond. In all these cases the disorder seems related to a collective motion involving more than one hydrogen bond at the same time, in analogy with circular hydrogen bonding found in hydrated β -cyclodextrins.²³ A single case of solid-state dynamical disorder has been hypothesized for 2-methyl-1,3-diphenylpropanedione enol from ¹³C CP/MAS NMR data^{2b} though its crystal structure was not determined because of solid-state tautomerization to the diketo form. With this exception, it may be reasonably concluded that no definitive proof of 2-fold proton disorder has been so far given for crystals of β -diketone enols forming only the intramolecular hydrogen bond.

Notwithstanding, it has recently been suggested²⁴ that in DBM crystals the enolic proton undergoes a continuous dynamical exchange paralleled by rapid changes of the two C-O distances, changes undetectable by X-rays which would only give average oxygen positions. Such a hypothesis was mainly backed by the

(20) The only exception reported of a symmetrically located proton comes from the crystal structure of bis(*m*-bromobenzoyl)methane (Williams, D. E.; Dumke, W. L.; Rundle, R. E. *Acta Crystallogr.* **1962**, *15*, 627). In this case, however, the molecule is in a special position on a crystallographic *m* and the symmetry can be imputed to statistical occupational disorder of the two enol tautomers.

(21) Haddon, R. C. *J. Am. Chem. Soc.* **1980**, *102*, 1807.

(22) (a) Herbstein, F. H.; Kapon, M.; Reisner, G. M.; Lehman, M. S.; Kress, R. B.; Wilson, R. B.; Shiau, W. I.; Duesler, E. N.; Paul, I. C.; Curtin, D. Y. *Proc. R. Soc. London* **1985**, *A399*, 295. (b) Tonnesen, H. H.; Karlson, J.; Mostad, A. *Acta Chem. Scand.* **1982**, *B36*, 475. (c) Destro, R.; Marsh, R. E. *J. Am. Chem. Soc.* **1984**, *106*, 7269.

(23) (a) Betzel, C.; Saenger, W.; Hingerty, B. E.; Brown, G. M. *J. Am. Chem. Soc.* **1984**, *106*, 7545. (b) Steiner, T.; Mason, S. A.; Saenger, W. *J. Am. Chem. Soc.* **1990**, *112*, 6184.

(24) Vila, A. J.; Lagier, C. M.; Olivieri, A. C. *J. Chem. Soc. Perkin Trans.* **2** **1990**, 1615.

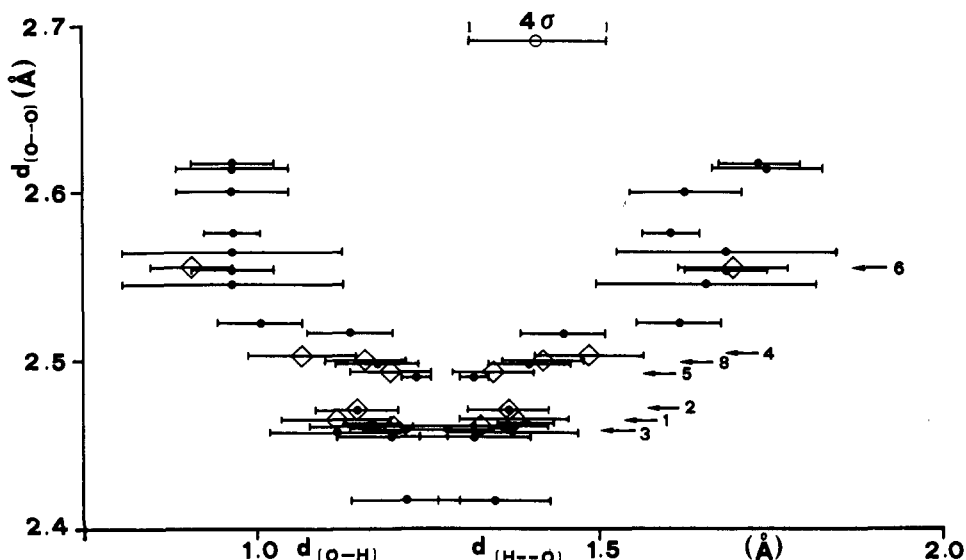


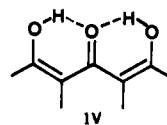
Figure 4. Scatter plot of $d(\text{O}-\text{O})$ vs $d(\text{O}-\text{H})$ and $d(\text{H}-\text{O})$ for the intramolecular hydrogen bond in compounds 1–6 and 8 (open squares) superimposed to the same scatter plot for the 18 β -diketone enols studied in our previous paper.¹ $d(\text{OH})$ standard deviations are indicated as $\pm 2\sigma$ bars.

results of AM1 semiempirical calculations. Apart from the questionable quality of the quantum mechanical calculations, which gave a $d(\text{O}-\text{O})$ value of 2.741 Å in total disagreement with the experimental value (2.460 (2), 2.460 (5), and 2.463 (4) Å by X-ray^{14b} and neutron^{14a} diffraction on the same crystal form and 2.452 (3) Å from X-rays on a different polymorph^{14c}), the idea of a fast exchange between two tautomers seems to be untenable in view of more basic diffraction physics considerations. The time of a single interaction of X-rays or neutrons with matter is extremely short (some 10^{-18} s²⁵), while a diffraction experiment takes a rather long period of time. This implies that the resulting structure is a weighted average of a large number of single interactions where dynamical motion will result in abnormally large thermal ellipsoids. In the present case the dynamical model would cause the two oxygens to have thermal ellipsoids elongated along the C–O bond, a kind of thermal motion never observed in any structure of DBM derivatives.

The enol proton tends to approach a symmetrical position when the O–O distance shortens, and extrapolation of $d(\text{O}-\text{H})$ and $d(\text{H}-\text{O})$ vs $d(\text{O}-\text{O})$ curves (Figure 4) indicates that it should be at the center for any $d(\text{O}-\text{O})$ shorter than some 2.43 Å. The fact that this never happens clearly corroborates the idea of some fundamental quantum mechanical reason preventing it (for instance the one suggested by Haddon²¹). It is interesting to note that a few substances having very short O–O distances appear to avoid a symmetrically positioned proton by cocrystallizing the two chemically different enol tautomers within the same asymmetric unit, as exemplified by compound 7, where the two tautomers have $d(\text{O}-\text{O})$ of 2.432 (4) or 2.434 (4) Å, and by usnic acid,²⁶ where $d(\text{O}-\text{O})$ is 2.40 and 2.41 Å for the two isomers.

Two independent factors appear to affect which side of the molecule the proton resides on in molecules where R_1 and R_3 (IIa) are chemically nonequivalent. The first concerns the relative electronegativities of R_1 and R_3 . Comparison of the few crystal structures of dissymmetrically substituted β -diketones ($R_1, R_3 = \text{H, alkyl};^{27a} \text{COOMe, Me};^{27b} \text{CF}_3, 1\text{-thienyl};^{27c}$ and Ph, Me^{27d})

shows that the proton chooses the oxygen atom on the side of the molecule that has the more electronegative substituent, in agreement with the spectroscopic results⁹ discussed in the introduction. This is confirmed by the structures of the three β -keto esters and of the only β -keto amide enols,^{27e–g} all having the proton on the opposite side of the esteric or amidic function. The second factor arises from other additional inter- or intramolecular hydrogen bonds involving the two oxygens of the keto-enol system. Experimental data show that, in the three known structures^{28a–c,2d} where the β -diketone enol is the acceptor of multiple hydrogen bonds, the extra proton donors always bond to the carbonyl oxygen. Accordingly, in doubly enolized β, β' -triketones (1,3,5-pentane-triones), IV, the carbonyl group is the acceptor for both intramolecular hydrogen bonds.^{28d–g}



In the present compounds the electronegativities of the different phenyl substituents can be evaluated by their Hammett constants: Me, $-0.07, -0.15, -0.05, -0.10$; OMe, $0.12, -0.27, 0.31, -0.41$; NO₂, $0.71, 0.78, 0.70, 0.10$ for $\sigma_m, \sigma_p, \sigma_1,$ and σ_R , respectively.²⁹ The *p*-methoxy groups are always found on aromatic rings which are essentially coplanar with the enol fragment, so a σ_p of -0.27 is the best Hammett constant to be used for this group. The *o*-NO₂ in compound 6 has a charge transfer interaction with the C(2) carbonyl atom and the Hammett constant alone may not be a good measure of the electron-donating ability of this group. With this in mind and on a qualitative basis, compounds 2, 3, 4, 6, and 8 are seen to conform to the rule that the proton is on the side of the more electronegative substituent.

By contrast, in compounds 1 and 5 the proton is on the wrong side as far as the application of this simple rule is concerned. It is not difficult to show, however, that these exceptions are a consequence of multiple C–H–O contacts to the two oxygens

(25) Muetterties, E. L. *Inorg. Chem.* **1965**, *4*, 769.

(26) Norrestam, R.; von Glehn, M.; Vachmeister, C. A. *Acta Chem. Scand. Ser. B* **1974**, *28*, 1149.

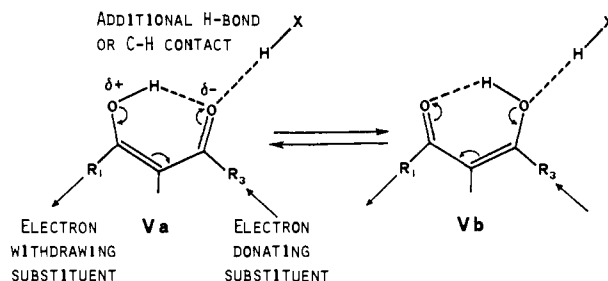
(27) (a) Barash, I.; Manulis, S.; Kashman, Y.; Springer, J. P.; Chen, M. H. M.; Clardy, J.; Strobel, G. A. *Science* **1983**, *220*, 1065. (b) Sheldrick, W. S.; Trowitzsch, Z. *Naturforsch. Teil B* **1983**, *38*, 220. (c) Jones, R. D. G. *Acta Crystallogr. Sect. B* **1976**, *32*, 1224. (d) Semmingsen, D. *Acta Chem. Scand.* **1972**, *26*, 143. Jones, R. D. G. *Acta Crystallogr. Sect. B* **1976**, *32*, 2133. (e) Saha, B.; Roy, S. C.; Satyanarayana, G. O. S. V.; Ghatak, U. R.; Seal, A.; Ray, S.; Bandyopadhyay, R.; Gosh, M.; Das, B.; Basak, B. S. *J. Chem. Soc. Perkin Trans. 1* **1985**, 505. (f) Egorov, M. P.; Bel'skii, W. K.; Petrov, E. S.; Terekhova, M. I.; Beletskaya, I. P. *Zh. Org. Khim.* **1984**, *20*, 2033. (g) Kornis, G.; Marks, P. J.; Chidester, C. G. *J. Org. Chem.* **1980**, *45*, 4860.

(28) (a) Tonnesen, H. H.; Karlsen, J.; Mostad, A.; Pedersen, U.; Rasmussen, P. B.; Lawesson, S. O. *Acta Chem. Scand. Ser. B* **1983**, *37*, 179. (b) Karlsen, J.; Mostad, A.; Tonnesen, H. H. *Acta Chem. Scand. Ser. B* **1988**, *42*, 23. (c) Simonsen, O.; Thorup, N. *Acta Crystallogr. Sect. B* **1979**, *35*, 432. (d) Cea-Olivares, R.; Rodriguez, I.; Rosales, M. J.; Toscano, R. A. *Aust. J. Chem.* **1987**, *40*, 1127. (e) O'Connell, M. J.; Ramsay, C. G.; Steel, P. J. *Aust. J. Chem.* **1985**, *38*, 401. (f) Thailanbal, V. G.; Pattabhi, V.; Gabe, E. J. *Acta Crystallogr. Sect. C* **1986**, *42*, 1017. (g) Casellato, U.; Graziani, R.; Mac-carone, G.; Purello, R. R.; Vidali, M. *J. Cryst. Spectrosc. Res.* **1987**, *17*, 323. (29) Exner, O. In *Advances in Linear Free Energy Relationships*; Chapman, N. B., Shorter, J., Eds.; Plenum Press: London, 1972; Chapter 1.

inside the crystal. These effects can be quantified by computing the sums of *bond valences*, s ,³⁰ for all C—H—O interactions involving the two oxygens, $\sum s(\text{C}=\text{O})$ and $\sum s(\text{C}-\text{OH})$, where any single contribution s is calculated as $s = \exp[(R_0 - R)/B]$, B and R_0 being semiempirical parameters for the O—H interactions having values of 0.37 and 0.88 Å, respectively,^{30c} and R being the actual O—O contact distance. The contribution of the enol proton was not included and final values of $\sum s(\text{C}=\text{O})$ and $\sum s(\text{C}-\text{OH})$ are given in the last columns of Table III together with their relative differences, $\Delta \Sigma$. As expected, the larger positive $\Delta \Sigma$ values are associated with compounds 1 and 5 (0.015 and 0.016, respectively) showing that the weak C—H—O interactions can exert effects similar to those produced by a single additional hydrogen bond (IV). Of course, no justification can be found in these terms for crystal 7 containing *both* enol tautomers. Since this compound displays by far the shortest O—O distances (2.434 (4) and 2.432 (4) Å), the reason for the dissymmetry has to be imputed to the already quoted second-order Jahn–Teller effect.²¹

A general understanding of the reasons why one oxygen may be chosen by the proton instead of the other one (or, in homology, one carbonyl enolizes more easily than the other) can be obtained in the frame of the RAHB model by saying that the energetically more stable isomer is the one for which resonance can generate the larger negative or positive partial charges on the carbonyl or hydroxyl oxygens, respectively, because this situation is inevitably associated with the stronger intramolecular hydrogen bond. In V the oxygen on the right would have a greater negative charge induced by both R_1 and R_3 as well as by the polarization effects caused by the additional X—H—O=C hydrogen bonds or short contacts. Thus Va should be the preferred configuration with respect to Vb. It is important to stress, however, that apart from the proton localization problem, any strong electron-donating 1,3-substituent (such as OR or NR₂) or any further hydrogen bonding to the carbonyl group will be detrimental, per se, to the π delocalization. This is particularly evident in the comparison between β -diketone and β -keto ester or β -keto amide enols of known molecular structures ($0 \leq Q \leq 0.17$ Å and $2.40 \leq d(\text{O}-\text{O}) \leq 2.55$ Å in diketones and $0.17 \leq Q \leq 0.28$ Å and $2.52 \leq d(\text{O}-\text{O}) \leq 2.65$ Å in keto esters or amides)^{2d} but can be seen also in the cases of β -diketone enols forming an additional hydrogen bond,

as in IV, where $0.10 \leq Q \leq 0.15$ Å and $2.52 \leq d(\text{O}-\text{O}) \leq 2.63$ Å.



Conclusions

The RAHB model was introduced¹ to interpret the abnormally short $d(\text{O}-\text{O})$ distances occurring, in association with O=C=C—C=O π system delocalization, in intramolecularly hydrogen bonded β -diketone enols. The present determination of the crystal structures, IR $\nu(\text{OH})$ stretching frequencies, and ¹H NMR chemical shifts of the enolic proton in eight new 1,3-diaryl-1,3-propanedione enols shows that these compounds conform to the proposed model as far as O—O distances, π delocalization (measured by the Q antisymmetrical vibration coordinate), $d(\text{O}-\text{H})$ values and estimates of the maximum intramolecular hydrogen bond energies (some 70 kJ mol⁻¹) are concerned. Furthermore, the model appears to be able to interpret fine structural details such as the general weakening of the intramolecular hydrogen bond caused by electron-donating 1,3-substituents or additional hydrogen bonds accepted by the carbonyl and the less favored enolization of the carbonyl group with the higher negative partial charge on its oxygen atom.

Acknowledgment. We are indebted to Prof. P. L. Caramella and Dr. T. Bandiera (University of Pavia) for having provided the crystals and for useful discussion, Dr. F. Stasi and Prof. C. Giacobozzo (University of Bari) for helping us in using the SIR88 system of direct methods programs, and Mr. G. Bertocchi for technical help. This research has been financially supported by the MPI(40%), Rome.

Supplementary Material Available: Tables of positional parameters, anisotropic temperature factors, and complete listings of distances and angles for 1–8 (44 pages); tables of observed and calculated structure factors for 1–8 (67 pages). Ordering information is given on any current masthead page.

(30) (a) Pauling, L. *J. Am. Chem. Soc.* **1929**, *51*, 1010. (b) Brown, I. D.; Shannon, R. D. *Acta Crystallogr. Sect. A* **1973**, *29*, 266. (c) Brown, I. D.; Altermatt, D. *Acta Crystallogr. Sect. B* **1985**, *41*, 244.